Journal of
Composites Science

MDPI

Article

Core–Shell Inorganic/Organic Composites Composed of Polypyrrole Nanoglobules or Nanotubes Deposited on MnZn Ferrite Microparticles: Electrical and Magnetic Properties

Marek Jurča [1], Lenka Munteanu [1], Jarmila Vilčáková [1], Jaroslav Stejskal [1,2,*], Miroslava Trchová [2], Jan Prokeš [3] and Ivo Křivka [3]

[1] University Institute, Tomas Bata University in Zlin, 760 01 Zlin, Czech Republic; jurca@utb.cz (M.J.); strouhalova@utb.cz (L.M.); vilcakova@utb.cz (J.V.)
[2] Central Laboratories, University of Chemistry and Technology, 166 28 Prague, Czech Republic; miroslava.trchova@vscht.cz
[3] Faculty of Mathematics and Physics, Charles University, 180 00 Prague, Czech Republic; jprokes@semi.mff.cuni.cz (J.P.); krivka@semi.mff.cuni.cz (I.K.)
* Correspondence: stejskal@utb.cz

Abstract: Core–shell inorganic/organic composites have often been applied as fillers in electromagnetic interference shielding. Those composed of conducting polymers and ferrites are of particular interests with respect to their electrical and magnetic properties. Pyrrole was oxidized in aqueous medium in the presence of manganese-zinc ferrite microparticles with ammonium peroxydisulfate or iron(III) chloride to yield polypyrrole-coated, core–shell microstructures. The effect of methyl orange dye on the conversion of globular polypyrrole to nanotubes has been demonstrated by electron microscopy when iron(III) chloride was used as an oxidant. The formation of polypyrrole was proved by FTIR spectroscopy. The completeness of ferrite coating was confirmed by Raman spectroscopy. The resistivity of composite powders was determined by four-point van der Pauw method as a function of pressure applied up to 10 MPa. The conductivity of composite powders was determined by a polypyrrole matrix and only moderately decreased with increasing content of ferrite. The highest conductivity of composites, 13–25 S cm^{-1}, was achieved after the deposition of polypyrrole nanotubes. Magnetic properties of composites have not been affected by the polypyrrole moiety, and the magnetization of composites was proportional to the ferrite content.

Keywords: conducting polymer; conductivity; resistivity; ferrite microparticles; hybrid composite; globular polypyrrole; polypyrrole nanotubes; magnetic properties

Citation: Jurča, M.; Munteanu, L.; Vilčáková, J.; Stejskal, J.; Trchová, M.; Prokeš, J.; Křivka, I. Core–Shell Inorganic/Organic Composites Composed of Polypyrrole Nanoglobules or Nanotubes Deposited on MnZn Ferrite Microparticles: Electrical and Magnetic Properties. *J. Compos. Sci.* **2024**, *8*, 373. https://doi.org/10.3390/jcs8090373

Academic Editor: Francesco Tornabene

Received: 28 August 2024
Revised: 14 September 2024
Accepted: 19 September 2024
Published: 21 September 2024

1. Introduction

The composites are composed at least of two components that provide functional properties associated with their specific microstructure. Hybrid organic/inorganic composites are often based on magnetic and conducting inorganic microparticles embedded in a matrix of organic polymer that enables the processing and affords mechanical properties required by applications. The use of organic conducting polymers introduces an additional functional moiety into the composite. Conducting polymers are typically represented in hybrid composites by polyaniline and polypyrrole, and their inorganic part by metals, metal oxides, and sulfides or ferrites [1]. The combination of electrical and electrochemical properties afforded by the former component with magnetic ones of inorganic part has often been used in the design of new functional materials. The papers on this topic started to appear only in the beginning of this century [2,3] and their number increased in following years. The present contribution concentrates on the recent advances in hybrid polypyrrole/ferrite composites and their experimental extension.

The composites comprising polypyrrole and ferrites are the best examples of promising functional materials [4]. They have been prepared simply by mixing of both

components [5–9]. Usually, however, the in-situ coating of ferrite with polypyrrole has been exploited as it guarantees more intimate interaction between the components and even distribution of inorganic part in an organic matrix. As a rule, polypyrrole was prepared by the oxidation of pyrrole in aqueous medium containing dispersed ferrite nanoparticles or microparticles [10–18]. In this way, ferrite particles become coated with an overlayer of conducting polymer thus creating core–shell microstructure [2,12,15]. The process is based on the generation of pyrrole oligomers that adsorb at the dispersed particles followed by the brush-like growth of polypyrrole chains from the surface. In the resulting composite, ferrite microparticles are dispersed in polypyrrole matrix. They are separated by the coating and cannot be in contact with each other, in contrast with mixtures where they form clusters. The composites are obtained as powders. They can be applied directly compressed to pellets or, depending on the intended application, they are embedded as fillers in inert polymer matrix that affords the desired form and mechanical properties [8].

Polypyrrole can be present in two fundamental morphologies at nanoscale, as nanoglobules or nanotubes. The latter form is obtained when the preparation of polypyrrole is carried out in the presence of methyl orange dye [19,20] that acts as a structure-guiding agent. Nanotubes are preferred over the globular form when the conductivity higher by one order of magnitude is of benefit.

Ferrite nanoparticles or microparticles used in the literature for the deposition of polypyrrole have been based on barium [7,9,14,21–24], cobalt [2,25–28], magnesium [10], manganese [13,29,30], manganese-zinc [3,11,15,31,32], nickel [12,33], strontium [6], or zinc [8,16–18,26,34]. A closely related magnetite is not included in this brief account.

Ternary composites including the third component, usually an organic elastomer, have also been reported. Auxiliary polymer additives, e.g., gelatin [22,23], alginate [16], or polyurethane [31], served to improve the composite processing or to provide the specific microstructure required by applications. The preparation protocol may include additional inorganic components based mainly on carbon, viz. graphene [29], graphite nitride [34], graphite oxide [25,27,32], or carbon nanotubes [35], usually in order to improve the conductivity.

Many applications of polypyrrole/ferrite composites have been based on both electrical and magnetic properties. Ferrites are typical ferromagnetic components in materials used for the shielding of electromagnetic interference [6,9,12,36]. Polypyrrole introduces the conductivity. Therefore, the radiation reflection and absorption contributions can be conveniently balanced by the composite composition [12,14,21]. The microwave absorption by both components has been used in the heating elements for the hyperthermia treatment of tumours in medicine [5,13].

Magnetic properties alone play a key role in magnetorheological fluids when the rheology of particles suspension is controlled by applied magnetic field. In this case, regardless of the conductivity, conducting polymer coating reduces the average particle density and prevents the sedimentation and aggregation of magnetic particles [37]. When polypyrrole is used as a coating in the core–shell structure, the interfacial phenomena between the ferrite core and polypyrrole coating may also occur [34,38] resulting in the change of magnetic properties. Polypyrrole may also act as an efficient adsorbent in water pollution treatment [39,40]. In the composites with ferrites, it has been used for removal of pollutant organic dyes [8,23,32], drugs [16], and chromium(VI) [22]. Ferrite allows for the separation and recovery of adsorbent by magnetic field.

The electrochemical activity of polypyrrole in the composites with ferrites has been exploited in energy-storage devices, such as supercapacitors [41]. The copper-cobalt ferrite coated with a conducting polymer served as an electrode [42]. Polypyrrole then provides pseudocapacitance contribution [25,27–29,33]. In lithium-ion batteries, polypyrrole/zinc ferrite electrodes displayed improved conductivity and stability during long-term cycling [17,18]. Electrochemical properties of polypyrrole manifest themselves in the corrosion protection. For example, polypyrrole/barium ferrite composite was tested in the

corrosion inhibition of aluminium [21]. In another field, electrochemically driven release of simazine herbicide was proposed [35].

Catalytic properties of composites are also valued. For example, ferrite coated with polypyrrole was applied as an electrocatalyst in oxygen evolution reaction [43]. In addition, the composites participated in the photocatalysis of hydrogen evolution [26,34] or assisted in photodegradation of ciprofloxacin antibiotics [34].

As illustrated above, functional polypyrrole/ferrite composites have been used in widely differing applications. The studies of their microstructure and fundamental electrical, magnetic, and physico-chemical properties are thus essential to understand their role and performance. Despite the explicit or implicit use of electrical conductivity, the quantitative assessment of this parameter is missing in the literature. This is partly due to the experimental difficulties met with the characterization of powders that cannot be compressed to pellets needed for routine four-point conductivity measurement. Moreover, the measured quantity is dependent on applied pressure.

The present study concentrates on hybrid composites composed of polypyrrole-coated MnZn ferrite. Electrical properties afforded mainly by polypyrrole are of prime interest. The feasibility of the coating of MnZn ferrite with polypyrrole has already been reported in the literature [3,15,31,32]. The present study extends the protocol of polypyrrole preparation, viz. the effect of acidity of reaction medium and oxidant type. It also concentrates on the generation of polypyrrole in both globular and nanotubular forms. The evaluation of electrical properties of composite powders as a function of applied pressure is newly reported. The core–shell composites of are designed for the application as fillers in electromagnetic interference shielding and they will be tested for this purpose in forthcoming studies.

2. Materials and Methods

2.1. Preparation

Microparticles with average size 11 μm of manganese-zinc (MnZn) ferrite (Siferrit material N27, TDK Electronics s.r.o., Czech Republic) with the morphology of irregular crushed particles was used as a substrate for the coating with a conducting polymer. Various amounts of ferrite (1–8 g) were dispersed in water containing pyrrole, and ammonium peroxydisulfate solution in water or 0.1 M sulfuric acid was added to start in situ polymerization of pyrrole at room temperature. The 200 mL of reaction mixture contained 0.1 M pyrrole (1.34 g, 20 mmol) and 0.125 M ammonium peroxydisulfate (5.71 g, 25 mmol). After 30 min, the ferrite microparticles coated with polypyrrole were separated on paper filter, and rinsed with water followed by ethanol to remove any unreacted species and soluble by-products. The solids containing also accompanying globular polypyrrole were dried at room temperature in open air.

The analogous composites were also prepared following the modified protocol in water that contained in addition 0.004 M methyl orange (260 mg) in attempt to promote the formation of polypyrrole nanotubes [19]. The syntheses have been carried out also with iron(III) chloride as an oxidant. In this case, 200 mL of reaction mixture contained 0.25 M iron(III) chloride hexahydrate (13.5 g, 50 mmol). All chemicals were supplied by Sigma-Aldrich branch (Prague, Czech Republic) and used as delivered.

2.2. Composition and Morphology

The weight fraction of ferrite was determined after the combustion of the organic part in oxygen at 800 °C in a muffle furnace (Nabertherm L9/S27, Lilienthal, Germany). Scanning electron microscope (Nova NanoSEM FEI, Brno, Czech Republic) was used to reveal the morphology of ferrite before and after the coating with polypyrrole.

2.3. Spectroscopy

ATR FTIR spectra were collected with a spectrometer Nicolet 6700 (Thermo-Nicolet, Waltham, MA, USA) using a reflective ATR extension GladiATR (PIKE Technologies, Fitch-

burg, WI, USA). Spectra were registered in the range of 4000–400 cm^{-1} with a resolution 4 cm^{-1}, 64 scans, and Happ-Genzel appodization.

Dispersive Raman spectra were registered in a back-scattering geometry using a Scientific DXR Raman microscope (Thermo Fisher Scientific, Waltham, MA, USA) with a 780 nm laser excitation line. The scattered light was analysed by a spectrograph with holographic grating 1200 lines mm^{-1} and a 50 µm pinhole width.

2.4. Electrical and Magnetic Properties

A lab-made press using a four-point van der Pauw setup was based on a cylindrical glass cell with an inner diameter of 10 mm [44] (Figure 1). The powdered composites were placed between a support and a glass piston with four electrodes at its perimeter. A Keithley 220 current source, a Keithley 2010 multimeter and a Keithley 705 scanner with a Keithley 7052 matrix card (Keithley Instruments Inc., Cleveland, OH, USA) were included in the setup. The pressure exerted with an E87H4-B05 stepper motor (Haydon Switch & Instrument Inc., Waterbury, CT, USA) up to 10 MPa (=102 kp cm^{-2}) limit was recorded with a L6E3 strain gauge cell (Zemic Europe BV, Etten-Leur, The Netherlands). The sample thickness was monitored with a dial indicator Mitutoyo ID-S112X (Mitutoyo Corp., Sakado, Japan). The resistivity of composites was also separately determined on pellets prepared at 527 MPa with a manual hydraulic press (Specac, Orpington, UK).

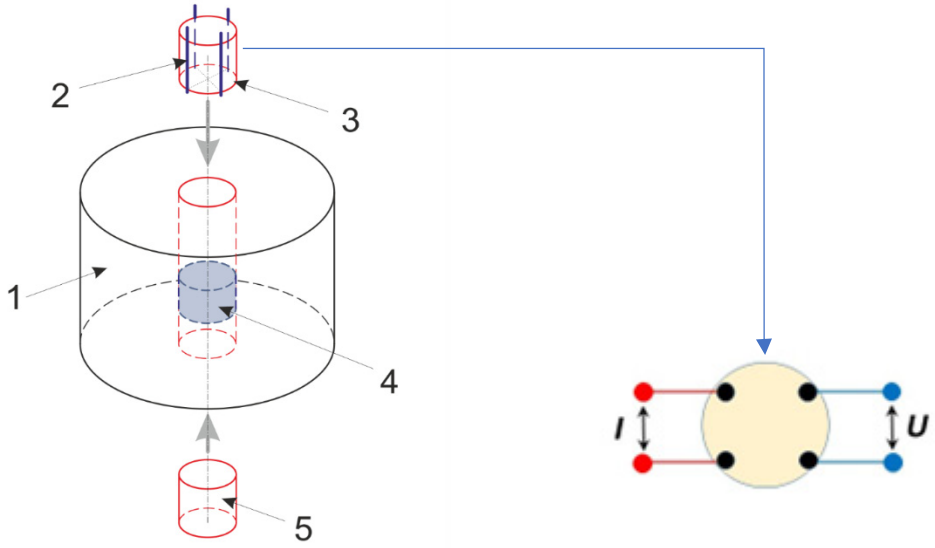

Figure 1. Four-point van der Pauw method of conductivity determination: 1—glass cylinder, 2—platinum/rhodium contact wires, 3—glass piston with incorporated platinum electrodes, 4—powder sample, 5—glass support. The DC voltage, *U*, was applied on the tip electrodes placed on the perimeter of the cylindrical sample base and the passing current, *I* (parallel with the bases) was recorded. Potential polarization effects and inhomogeneity issues were reduced by switching of electrodes.

Magnetic hysteresis curves were determined at room temperature in the range ±10 kOe by a vibrating sample magnetometer (VSM, Model 7407, Westerville, OH, USA).

3. Results and Discussion

3.1. Composites

Conducting polymers are prepared by the chemical or electrochemical polymerization of respective monomers. The former takes place in water and exploits a variety of inorganic oxidants. In the present study, the oxidation of pyrrole to polypyrrole used the most common ammonium peroxydisulfate [11,12,15,26] and iron(III) chloride [13,18] (Figure 2). The ferrite surfaces immersed in the aqueous reaction mixture become coated with thin polymer films of submicrometer thickness [45]. The hydrophobic oligomers generated in the early stages of monomer oxidation adsorb at available interfaces and initiate the

brush-like growth of polymer chains. This results in the coating of ferrite microparticles with polypyrrole. Any polypyrrole produced outside ferrite microparticles accompanies them, and the final product is thus composed of core–shell, polypyrrole-coated ferrite microparticles dispersed in polypyrrole matrix (Figure 2).

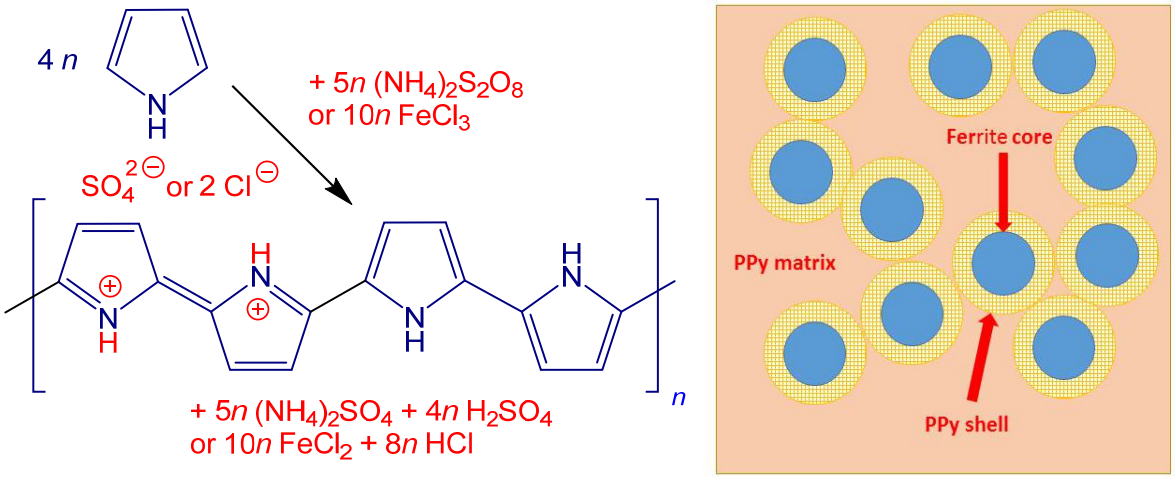

Figure 2. The oxidation of pyrrole in aqueous medium yields polypyrrole sulfate or chloride. Ferrite microparticles become coated with polypyrrole (PPy) shell, and are embedded in the matrix of accompanying conducting polymer.

Three series of polypyrrole coatings of MnZn ferrite were tested. (1) The oxidation of pyrrole with ammonium peroxydisulfate in water, (2) in acidic medium of 0.1 M sulfuric acid, and (3) the oxidation of pyrrole with iron(III) chloride hexahydrate. The syntheses in each series have been carried out in the absence or in the presence of methyl orange that was expected to alter polypyrrole morphology. In the former case, globular polypyrrole is obtained while the organic dye supports the formation of polypyrrole nanotubes, which have higher conductivity [19,20,46].

3.2. Composition and Morphology

Various amounts of ferrite have been added to the reaction mixture (Section 2.1, Table 1). The idealized stoichiometry (Figure 2) expects the 1.78 g yield of polypyrrole sulfate. If, for example, x g of ferrite were added, the predicted content of ferrite in the composite would be $x/(1.78 + x)$, in good agreement with experimental results (Table 1). This means that that ferrite acts as an inert additive that does not affect the chemistry of synthesis and serves as a template for coating only. This is not automatically satisfied. For instance, in the similar experiments with the coating of nickel microparticles with polyaniline or polypyrrole, nickel dissolved in part or even completely depending under such reaction conditions [47].

Table 1. Content of ferrite (wt%) in the composites with globular polypyrrole prepared in various media using ammonium peroxydisulfate (APS) or iron(III) chloride ($FeCl_3$) oxidants in 200 mL of reaction mixture containing g grams MnZn ferrite.

g, g MnZn Ferrite	Expected (Figure 2)	Water/APS	0.1 M H_2SO_4/APS	Water/$FeCl_3$
1	35.9	32.6	31.7	–
2	52.9	52.5	44.6	52.0
4	69.2	68.3	64.2	–
6	77.1	76.5	72.2	76.7
8	81.7	81.5	78.7	81.4

The morphology of ferrite resembles a crushed stone-like material (Figure 3) with particles of irregular shape, and particle size of units to tens micrometers with a broad size distribution. The original particles are accompanied by free polypyrrole (Figure 4). Some polypyrrole globules also adhere to the coating.

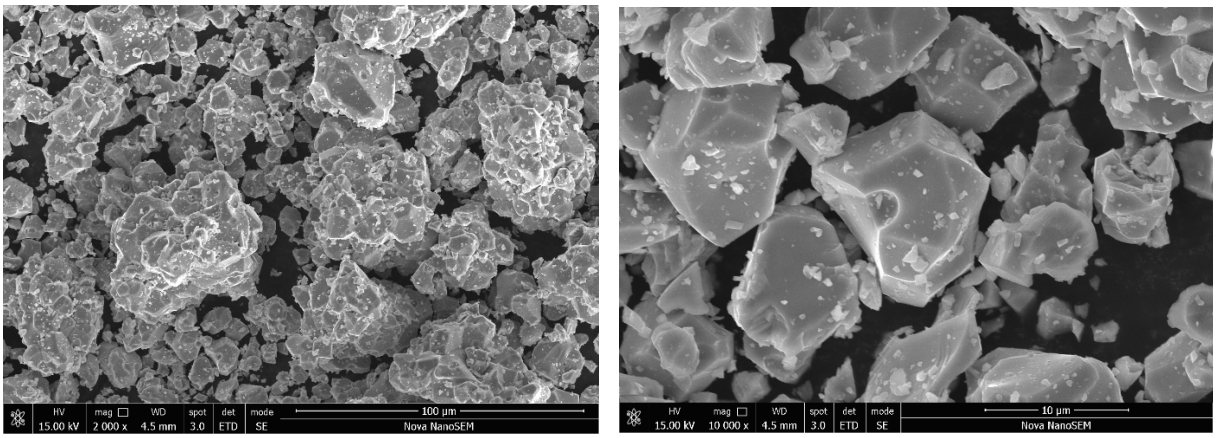

Figure 3. MnZn ferrite: (**a**) Lower and (**b**) higher magnification. Scale bars 100 and 10 µm.

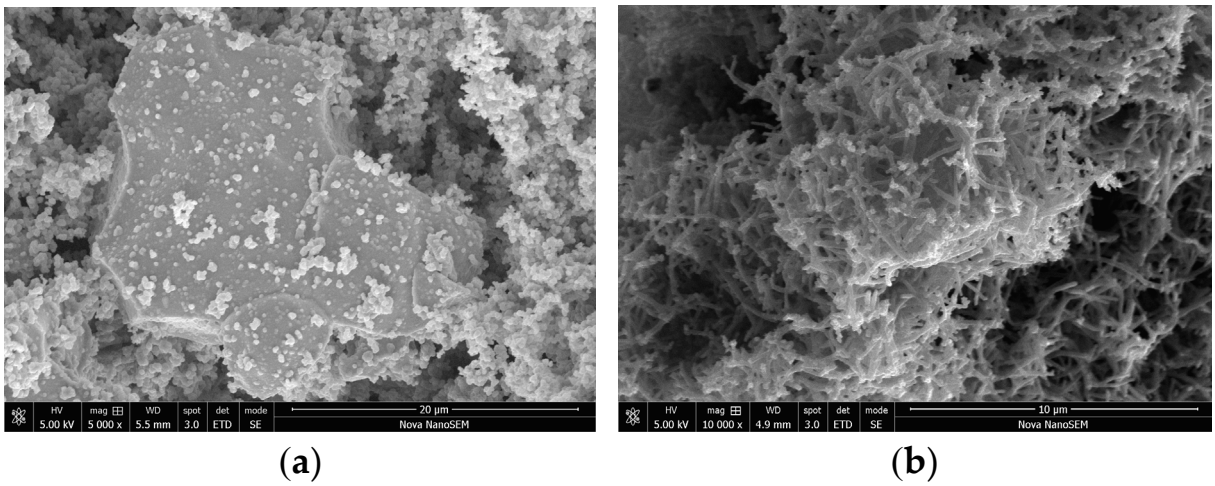

Figure 4. MnZn ferrite with deposited (**a**) globular polypyrrole and (**b**) polypyrrole nanotubes. The 200 mL of reaction mixture contained 2 g of ferrite. Scale bars 10 µm.

3.3. Spectroscopy

ATR FTIR spectrum of polypyrrole prepared in absence of ferrite (Polypyrrole in Figure 5a) corresponds to the protonated form of polypyrrole [46]. It exhibits the main bands with local maxima situated at 1540 cm^{-1} (C–C stretching vibrations in the pyrrole ring), 1458 cm^{-1} (C–N stretching vibrations in the ring), 1287 cm^{-1} (C–H and C–N in-plane deformation modes), 1161 cm^{-1} (breathing vibrations of the pyrrole ring), 1090 cm^{-1} (breathing vibrations of pyrrole ring), 1035 cm^{-1} (C–H and C–N in-plane deformation vibrations), 964 cm^{-1} (C–H out-of-plane deformation vibrations of the ring), and at the maxima at 768 and 664 cm^{-1} (C–C out-of-plane deformation vibrations of the ring) [47]. A maximum at 1695 cm^{-1} was assigned to the carbonyl group created by the nucleophilic attack of water on pyrrole ring during the preparation [19]. The shape of spectra of polypyrrole/MnZn ferrites did not change with increasing amount of ferrite in the reaction mixture. A broad absorption polaron band at wavenumbers above 2000 cm^{-1} corresponds to the polarons within the chain structure, which act as charge carriers that are responsible for the

electrical conduction. This band is more pronounced for polypyrrole prepared in absence of ferrite. The presence of ferrite is demonstrated by a sharp peak situated at 519 cm^{-1} (Figure 5a), which becomes reduced as the amount of deposited polypyrrole increases.

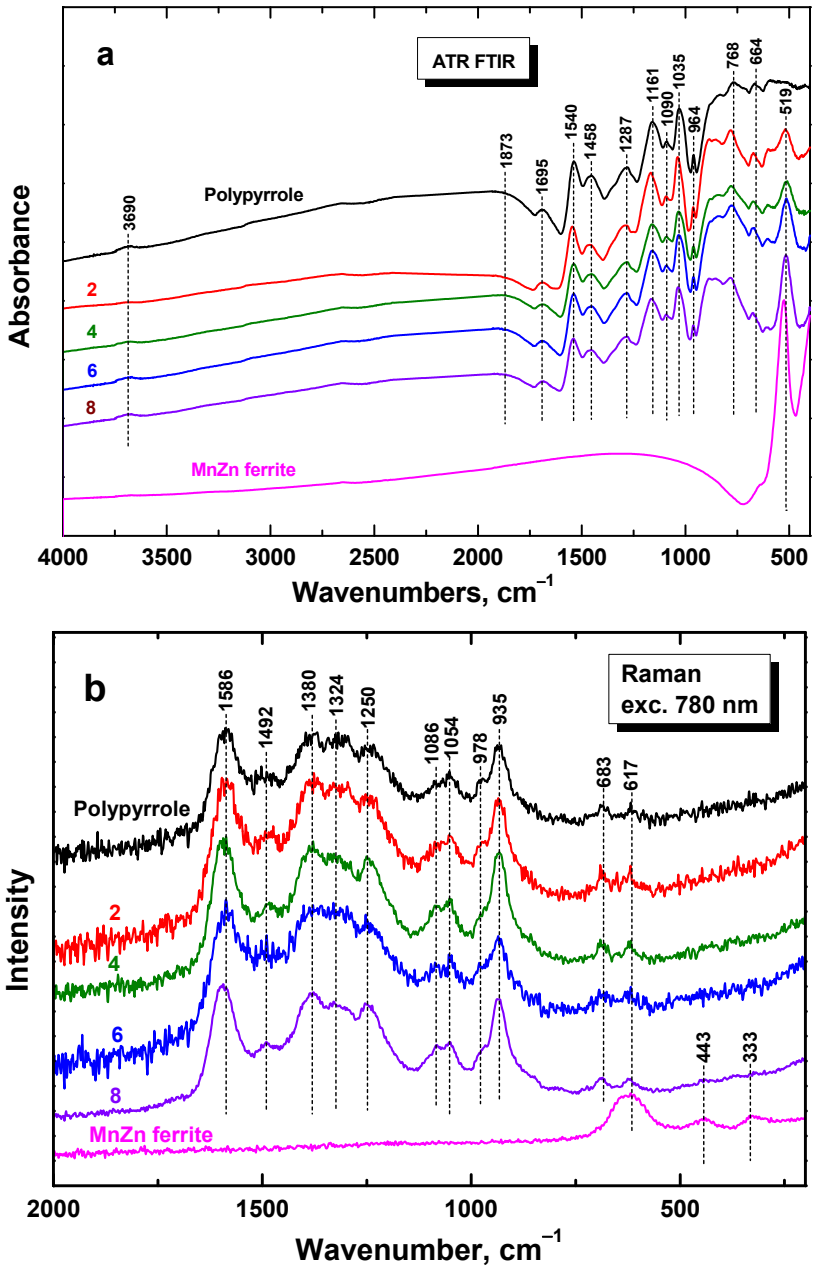

Figure 5. (**a**) FTIR and (**b**) Raman spectra of polypyrrole/MnZn ferrites for various amount if ferrite in the reaction mixture. The oxidation of pyrrole with ammonium peroxydisulfate in water with 0–8 g ferrite per 200 mL of reaction mixture.

Laser excitation wavelength 780 nm used in the Raman scattering is in resonance with the energy of polarons in the protonated polypyrrole. In Raman spectra of polypyrrole prepared in the absence of ferrite (Polypyrrole in Figure 5b), we detect the bands of polypyrrole with local maxima at 1586 cm^{-1} (C=C stretching vibrations of polypyrrole backbone) and 1492 cm^{-1} (C–C and C=N stretching skeletal vibrations), two bands of ring-stretching vibrations at 1380 and 1324 cm^{-1}, a band at 1250 cm^{-1} (antisymmetric C–H deformation vibrations), and a double-peak with local maxima at 1086 and 1054 cm^{-1} (C–H out-of-plane deformation vibrations, the second became sharper during

deprotonation [19,46]. The Raman spectroscopy is the method of the surface-sensitive characterization. Due to the resonance enhancement of the Raman spectrum of polypyrrole the presence of ferrite is not detected in the Raman spectra of ferrite/polypyrrole composites, thus confirming the complete coating of microparticles with conducting polymer.

3.4. Electrical Properties of Polypyrrole

The DC conductivity, or its reciprocal quantity, resistivity, is typically determined by the four-point method. Although the former parameter is somewhat favoured by physicists, the latter is often preferred by materials engineers. For powders, the determination is done with free-standing pellets prepared by the compression in hydraulic press. But not for all powders is this possible, with ferrites themselves being examples. In such cases, the resistivity must be then recorded as a function of pressure applied to powders, and the present experimental set-up allows for this type of measurements.

Electrical properties of polypyrrole depend on the conditions of polymer synthesis, e.g., the oxidant type and resulting morphology that can be affected by the presence of organic dyes [20], typically methyl orange (Figure 6). The double-logarithmic presentation of polypyrrole resistivity on pressure is about linear. Polypyrrole prepared with ammonium peroxydisulfate has higher resistivity that that produced with iron(III) chloride. Although the addition of methyl orange had marginal effect on resistivity with the former oxidant, it led to a marked decrease in the resistivity with the latter, i.e., the conductivity increased. This is the result of the conversion of globular morphology to nanotubes. An earlier study proved that with peroxydisulfate oxidant, the occurrence of nanotubes was rare, and they were always accompanied by the globular form [47], while with iron(III) chloride nanotubes clearly dominate [19] (Figure 4). The nanotubular morphology is thus responsible for the enhanced conductivity.

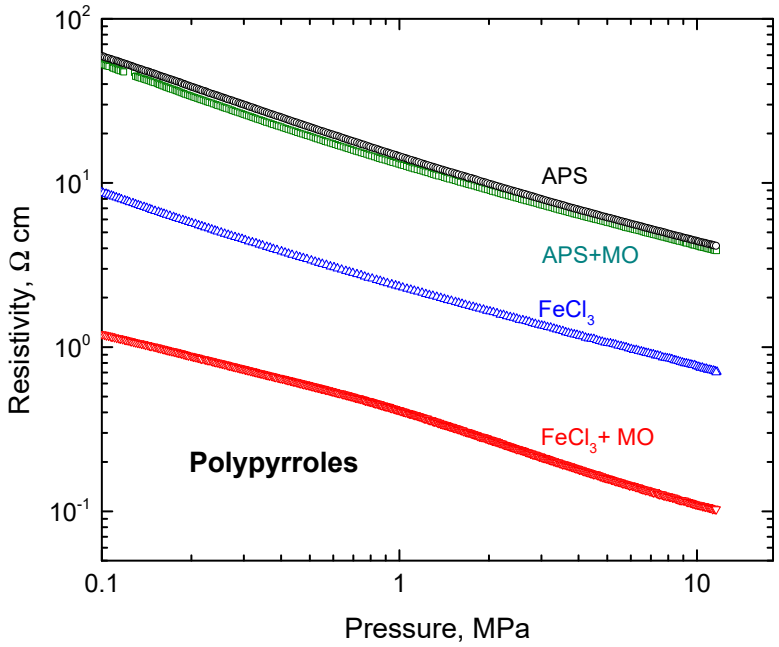

Figure 6. Pressure dependence of resistivity for polypyrroles prepared in water by the oxidation of pyrrole with ammonium peroxydisulfate or iron(III) chloride, in the absence or presence of methyl orange.

3.5. Electrical Properties of Polypyrrole-Coated Ferrites

Despite extensive studies of polypyrrole/ferrite composites, their DC conductivity has seldom been reported, and even then with widely differing results, from the order of 10^{-7} S cm^{-1} [6] to a high value of 120 S cm^{-1} [2], obviously depending on the ferrite type and the way of composite preparation. Typical conductivity of globular polypyrrole

established in the literature is of the order of units S cm^{-1} [19] and lower conductivity can be expected for ferrites. Six series of polypyrrole syntheses specified in the experimental part have been carried out to prepare polypyrrole-coated ferrites. The sample conductivities determined on compressed pellets are summarized in Table 2 with the following observations:

Table 2. Conductivity (S cm^{-1}) of polypyrrole/MnZn ferrite composites determined on pellets (prepared at 527 MPa pressure) for various mass, *g*, of MnZn ferrite in the reaction medium. Pyrrole was oxidized in water or 0.1 M H_2SO_4, with ammonium peroxydisulfate or iron(III) chloride, in the absence or presence of methyl orange (MO).

	Without Methyl Orange			With Methyl Orange		
***g*, MnZn Ferrite per 200 mL**	**APS/H_2O**	**APS/0.1 M H_2SO_4**	**$FeCl_3/H_2O$**	**APS/H_2O**	**APS/0.1 M H_2SO_4**	**$FeCl_3/H_2O$**
0 [a]	1.35	1.56	6.61	2.86	3.14	23.7
2	0.371	0.310	3.64	0.630	1.49	24.6
4	0.466	0.379	2.76	0.597	0.447	25.4
6	0.261	0.276	2.11	0.287	0.341	17.5
8	0.177	0.168	2.01	0.411	0.413	13.0

[a] Polypyrrole conductivity was taken from [47].

(1) The conductivity of composites moderately decreased with increasing content of ferrite in the samples. This is also easily visible in the corresponding resistivity vs. pressure curves (Figure 7). Please note that the resistivity of ferrite is four orders of magnitude higher compared to polypyrrole. As ferrite microparticles are coated with polypyrrole, the contact of ferrites cores is prevented (Figure 2), and the conductivity is determined exclusively by continuous polypyrrole matrix. The introduction of ferrite reduces the volume fraction of polypyrrole matrix in the composite and the resistivity only marginally increases in the response (Figure 7).

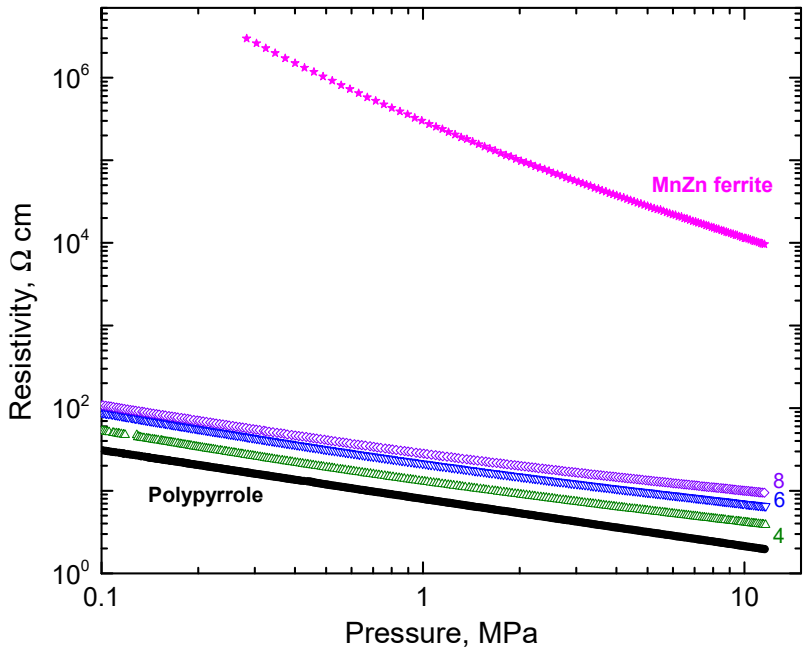

Figure 7. Pressure dependence of resistivity for polypyrrole/MnZn ferrite composites prepared in water by the oxidation of pyrrole with ammonium peroxydisulfate for various mass of ferrite, 0–8 g per 200 mL of reaction mixture.

Please note that the conductivity of filler particles does not matter. In fact, the same trend was obtained with the polypyrrole deposited on conducting nickel microparticles [47]. Because the metallic cores were protected by polypyrrole overlayer from mutual contacts, they cannot generate conducting nickel pathways. As an apparent paradox, the conductivity of composites surprisingly decreases with increasing nickel content due to the reduction of volume fraction of polypyrrole matrix, like in the present case with a MnZn ferrite.

(2) The increased acidity of the reaction medium by the addition of sulfuric acid had no influence on the conductivity of composites (Table 2). Polypyrrole composites prepared with peroxydisulfate had always lower conductivity compared with iron(III) chloride, but the differences were within one order of magnitude and are regarded as small. The introduction of methyl orange increased the conductivity only marginally with peroxydisulfate oxidant but significantly with iron(III) chloride in the response to the conversion of polypyrrole morphology.

3.6. Mechanical Properties

The present method of resistivity determination also allows for the monitoring of the change of sample thickness during the compression (Figure 8). The sample may be regarded as fluffy and easy to compress if these dependence in double-logarithmic presentations is steep. This is the case for polypyrrole alone (the slope −0.284). The introduction of ferrite led to a marginal reinforcement and the steepness was moderately reduced. Even at high ferrite loading, the mechanical properties were controlled mainly by polypyrrole matrix. Ferrite itself behaves as a practically incompressible material (slope −0.029) as expected. These observations are important for the application in magnetorheological suspensions where polypyrrole-coated ferrite would be better dispersible in the carrier medium than ferrites alone.

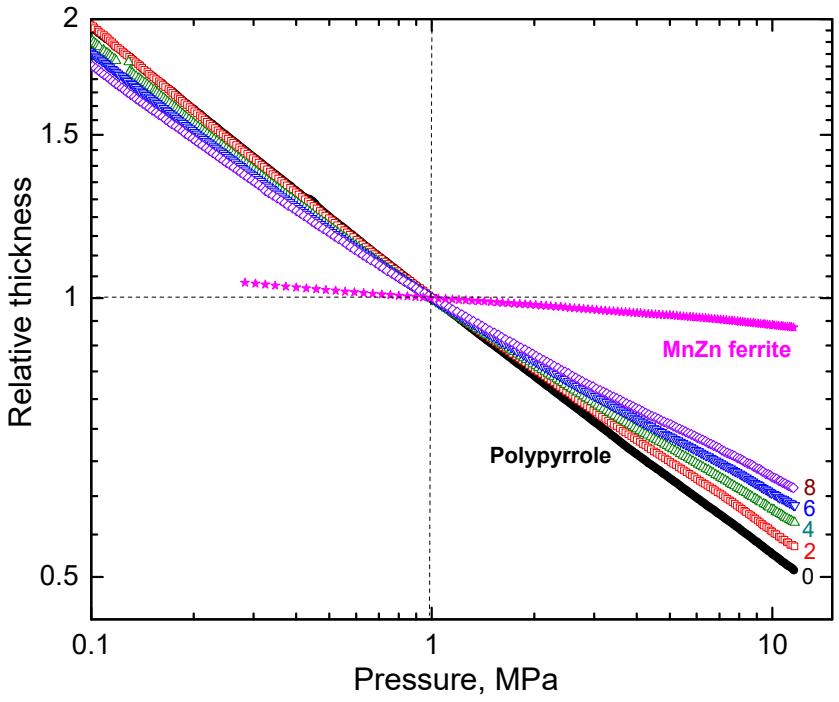

Figure 8. Pressure dependence of relative sample thickness for polypyrrole/MnZn ferrite composites shown in Figure 7.

3.7. Magnetic Properties

As expected, the highest magnetization 88.6 emu g^{-1}, (Table 3, Figure 9) was achieved with neat MnZn ferrite. Since polypyrrole itself does not display magnetic properties, the saturation and remanence magnetization of composite materials should be governed by

the amount of ferrite in the sample, which corresponds well with obtained values. From the coercivity and remanence values and the shape of the curve, it can be seen that the composites are magnetically soft materials as expected. No significant differences were observed for coercivity of the individual particles. The coating of ferrite with conducting polymer does not have any effect on the magnetostatic properties of ferrite cores. The analogous studies of MnZn ferrite coated with polyaniline [38,48], however, proved that the formation of a conducting polymer overlayer on the surface of a MnZn ferrite microparticles modified the character of the frequency dispersion of the magnetic permeability. The changes in the magnetic properties were due to the change of the boundary conditions of the microwave field at the interface between the ferrite particle and the polymer coating. Such effects are likely to occur also with polypyrrole-coated ferrite and they would become of importance when applied in electromagnetic interference shielding compositions.

Table 3. Coercivity, H_C, remanent magnetization, M_R, and saturation magnetization, M_S, of polypyrrole composites prepared with various amount of MnZn ferrite in water with ammonium peroxydisulfate oxidant.

g, g MnZn Ferrite	H_C, Oe	M_R, emu g^{-1}	M_S, emu g^{-1}
2	8.85	0.36	45.8
4	9.50	0.52	60.7
6	9.30	0.58	70.2
8	9.16	0.59	73.1
Ferrite	9.88	0.82	88.6

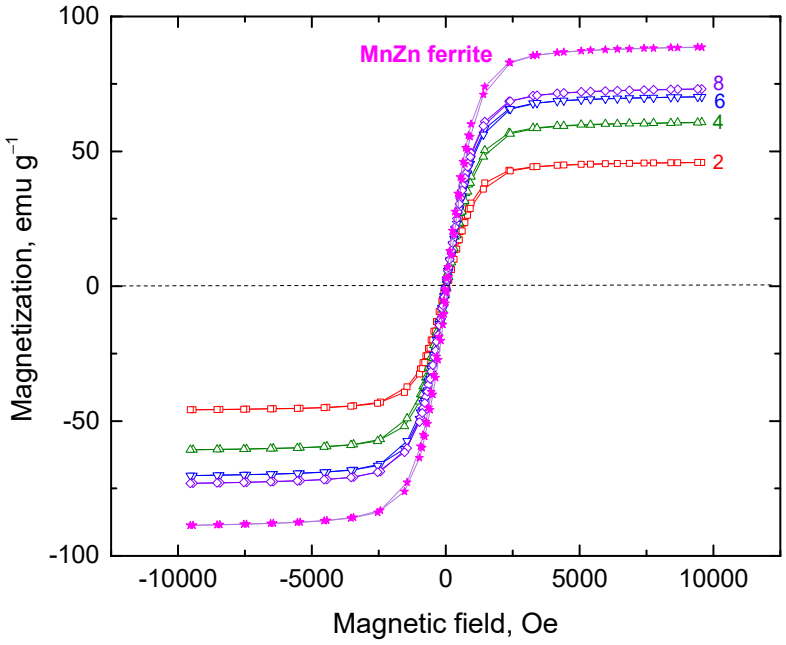

Figure 9. Magnetization curves of globular polypyrrole deposited on various amounts of ferrite microparticles 0–8 g per 200 mL of reaction mixture.

4. Conclusions

The study demonstrated the feasibility of the coating of manganese-zinc ferrite microparticles in situ during the oxidation of pyrrole with ammonium peroxydisulfate or iron(III) chloride in the presence or absence of methyl orange. The completeness of the coating was confirmed by Raman spectroscopy. When compressed to pellets, ferrite cores are separated from each other. They are embedded in a polypyrrole matrix, which determines

the conductivity. The conductivity of composites was therefore only moderately reduced with an increasing fraction of ferrite and stayed at the level of 10^{-1} S cm^{-1}. The conductivity was higher when iron(III) chloride was used as an oxidant instead of ammonium peroxydisulfate. Methyl orange dye used along with iron(III) chloride oxidant stimulated the growth of polypyrrole nanotubes and increased the conductivity of composites to 13–23 S cm^{-1}. The magnetostatic properties were determined by the presence of ferrite and the magnetization was proportional to the ferrite content. The hybrid polypyrrole-coated ferrites were designed as fillers for the electromagnetic interference shielding compositions to be analysed in the forthcoming study.

Author Contributions: M.J.: Methodology, data curation. L.M.: investigation. J.V.: methodology, supervision. J.S.: conceptualization, writing—review and editing. M.T.: validation, methodology. J.P.: investigation, data curation. I.K.: methodology, software. All authors have read and agreed to the published version of the manuscript.

Funding: This research was funded by the Ministry of Education, Youth and Sports of the Czech Republic (INTER-EXCELLENCE II LUAUS24032 and DKRVO RP/CPS/2024-28/005) and the Czech Science Foundation (22-25734S).

Data Availability Statement: The original contributions presented in the study are included in the article, further inquiries can be directed to the corresponding author.

Conflicts of Interest: The authors declare that they have no known competing financial interests or personal relationships that could have appeared to influence the work reported in this paper.

References

1. Saraswat, A.; Kumar, S. Cutting-edge applications of polyaniline composites towards futuristic energy supply devices. *Eur. Polym. J.* **2023**, *200*, 112501. [CrossRef]
2. Murillo, N.; Ochoteco, E.; Alesanco, Y.; Pomposo, J.A.; Rodriguez, J.; González, J.; del Val, J.J.; González, J.M.; Britel, M.R.; Varela-Feria, F.M.; et al. $CoFe_2O_4$-polypyrrole (PPy) nanocomposites: New multifunctional materials. *Nanotechnology* **2004**, *15*, S322–S327. [CrossRef]
3. Poddar, P.; Wilson, J.L.; Srikanth, H.; Morrison, S.A.; Carpenter, E.E. Magnetic properties of conducting polymer doped with manganese-zinc ferrite nanoparticles. *Nanotechnology* **2004**, *15*, S570–S574. [CrossRef]
4. Xiao, H.M.; Fu, S.Y. Synthesis and physical properties of electromagnetic polypyrrole composites via addition of magnetic crystals. *CrystEngComm* **2014**, *16*, 2097–2112. [CrossRef]
5. Hakeem, A.; Alshahrani, T.; Ali, I.; Alhossainy, M.H.; Khosa, R.Y.; Muhammad, G.; Khan, A.R.; Farid, H.M.T. Synthesis and characterization of composites for microwave devices. *Chin. J. Phys.* **2021**, *70*, 232–239. [CrossRef]
6. Khan, S.A.; Ali, I.; Hussain, A.; Javed, H.M.A.; Turchenko, V.A.; Trukhanov, A.V.; Trukhanov, S.V. Synthesis and characterization of composites with Y-hexaferrites for electromagnetic interference shielding applications. *Magnetochemistry* **2022**, *8*, 186. [CrossRef]
7. Aman, S.; Elsaeedy, H.I.; Alharbi, F.F.; Ejaz, S.R.; Ahmad, N.; Zeshan, M.; Ali, M.; Farid, H.T. Synthesis of composites and their characterization for high-frequency applications. *Inorg. Chem. Commun.* **2023**, *156*, 111188. [CrossRef]
8. Ashraf, A.; Munir, R.; Albasher, G.; Ghamkhar, M.; Muneer, A.; Yaseen, M.; Murtza, T.; Noreen, S. Utilization of $ZnFe_2O_4$-polyaniline (PANI), $ZnFe_2O_4$-polystyrene (PST), and $ZnFe_2O_4$-polypyrrole (PPy) nanocomposites for removal of Red X-GRL and Direct Sky Blue dyes from wastewater: Equilibrium, kinetic and thermodynamic studies. *J. Environ. Sci. Health A Toxic/Hazard. Subst. Environ. Eng.* **2023**, *58*, 914–934. [CrossRef]
9. Aman, S.; Ahmad, N.; Tahir, M.B. Synthesis and characterization of $BaGd_{0.075}Fe_{1.925}O_4$/polypyrrole composites for EMI shielding. *J. Mater. Sci. Mater. Electron.* **2024**, *35*, 35. [CrossRef]
10. Alburaih, H.A.; Khan, S.A.; Khosa, R.Y.; Ejaz, S.R.; Khan, A.R.; Muhammad, G.; Waheed, M.S.; Chughtai, A.H.; Manzoor, S.; Aman, S. The electrical, dielectric and magnetic effect of $MgFe_2O_4$-polypyrrole and its composites. *J. Korean Ceram. Soc.* **2022**, *60*, 357–363. [CrossRef]
11. Gabal, M.A.; Al-Harthy, E.A.; Al Angari, Y.M.; Awad, A.; Al-Juaid, A.A.; Hussein, M.A.; Abdel-Daiem, A.M.; Sobahi, T.R.; Saeed, A. Synthesis, structural, magnetic and high-frequency electrical properties of $Mn_{0.8}Zn_{0.2}Fe_2O_4$/polypyrrole core-shell composite using waste batteries. *J. Inorg. Organomet. Polym. Mater.* **2022**, *32*, 1975–1987. [CrossRef]
12. Guo, J.; Li, X.; Chen, Z.R.; Zhu, J.F.; Mai, X.M.; Wei, R.B.; Sun, K.; Liu, H.; Chen, Y.X.; Naik, N. Magnetic $NiFe_2O_4$/polypyrrole nanocomposites with enhanced electromagnetic wave absorption. *J. Mater. Sci. Technol.* **2022**, *108*, 64–72. [CrossRef]
13. Pyatakovich, F.A.; Mevsha, O.V.; Yakunchenko, T.I.; Makkonen, K.F.; Uvarov, V.M. Introducing a polypyrrole (PPy)-manganese ferrite ($MnFe_2O_4$) nanocomposite based microwave absorber for studying the effect of the radiation on the modification of the patient's functional state. *J. Nanostruct.* **2022**, *12*, 245–253. [CrossRef]

14. Darwish, K.A.; Hemeda, O.M.; Ati, M.I.A.; Abd El-Hameed, A.S.; Zhou, D.; Darwish, M.A.; Salem, M.M. Synthesis, characterization, and electromagnetic properties of polypyrrole-barium hexaferrite composites for EMI shielding applications. *Appl. Phys. A Mater. Sci. Proc.* **2013**, *129*, 460. [CrossRef]
15. Gabal, M.A.; Al-Harthy, E.A.; Al Angari, Y.M.; Awad, A.; Al-Juaid, A.A.; Saeed, A. Synthesis, characterization and electrical properties of polypyrrole/$Mn_{0.8}Zn_{0.2}Fe_2O_4$/GO ternary hybrid composites using spent Zn-C batteries. *J. Sol-Gel Sci. Technol.* **2023**, *15*, 781–792. [CrossRef]
16. Silva, E.C.; Soares, V.R.; Fajardo, A.R. Removal of pharmaceuticals from aqueous medium by alginate/polypyrrole/$ZnFe_2O_4$ beads via magnetic field enhanced adsorption. *Chemosphere* **2023**, *316*, 137734. [CrossRef]
17. Han, H.; Lou, Z.C.; Wang, Q.Y.; Xu, L.; Li, Y.J. Introducing rich heterojunction surfaces to enhance the high-frequency electromagnetic attenuation response of flexible fiber-based wearable absorbers. *Adv. Fiber Mater.* **2024**, *6*, 739–757. [CrossRef]
18. Jin, R.Y.; Liu, J.P.; Qiu, H.F.; Xu, C.; Weng, L.G.; Liu, C.B.; Zeng, Y. Synthesis of porous nanosheet-assembled $ZnFe_2O_4$@polypyrrole yolk-shell microspheres as anode materials for high-rate lithium-ion batteries. *J. Electroanal. Chem.* **2020**, *863*, 114038. [CrossRef]
19. Stejskal, J.; Trchová, M. Conducting polypyrrole nanotubes: A review. *Chem. Pap.* **2018**, *72*, 1563–1595. [CrossRef]
20. Stejskal, J.; Prokeš, J. Conductivity and morphology of polyaniline and polypyrrole prepared in the presence of organic dyes. *Synth. Met.* **2020**, *264*, 116373. [CrossRef]
21. Kadar, C.H.A.; Faisal, M.; Maruthi, N.; Raghavendra, N.; Prasanna, B.P.; Nandan, K.R.; Manohara, S.R.; Revanasiddappa, M.; Madhusudhan, C.K. Anticorrosive polypyrrole/barium ferrite (PPy/$BaFe_{12}O_{19}$) composites with tunable electrical response for electromagnetic wave absorption and shielding performance. *J. Electron. Mater.* **2023**, *52*, 2080–2093. [CrossRef]
22. Milakin, K.A.; Taboubi, O.; Hromádková, J.; Bober, P. Magnetic polypyrrole-gelatin-barium ferrite cryogel as an adsorbent for chromium (VI) removal. *Gels* **2023**, *9*, 840. [CrossRef] [PubMed]
23. Milakin, K.A.; Taboubi, O.; Acharya, U.; Lhotka, M.; Pokorný, V.; Konefal, M.; Kočková, O.; Hromádková, J.; Hodan, J.; Bober, P. Polypyrrole-barium ferrite magnetic cryogels for water purification. *Gels* **2023**, *9*, 92. [CrossRef] [PubMed]
24. Hosseinabad, T.; Nabiyouni, G.; Hedayati, K. Synthesis and characterization of structural, magnetic, and microwave properties of $Ba_{0.5}Sr_{0.5}Fe_{12}O_{19}$/$Ni_{0.5}Mn_{0.5}Fe_2O_4$/polypyrrole nanocomposite thin films. *J. Mater. Sci. Mater. Electron.* **2024**, *35*, 156. [CrossRef]
25. Mariappan, C.R.; Gajraj, V.; Gade, S.; Kumar, A.; Dsoke, S.; Indris, S.; Ehrenberg, H.; Prakash, G.V.; Jose, R. Synthesis and electrochemical properties of rGO/polypyrrole/ferrites nanocomposites obtained via a hydrothermal route for hybrid aqueous supercapacitors. *J. Electroanal. Chem.* **2019**, *845*, 72–83. [CrossRef]
26. Chamani, S.; Sadeghi, E.; Peighambardoust, N.S.; Doganay, F.; Yanalak, G.; Eroglu, Z.; Aslan, E.; Asghari, E.; Metin, O.; Patir, I.H. Photocatalytic hydrogen evolution performance of metal ferrites/polypyrrole nanocomposites. *Int. J. Hydrogen Energy* **2022**, *47*, 32940–32954. [CrossRef]
27. Ishaq, S.; Moussa, M.; Kanwal, F.; Ayub, R.; Van, T.N.; Azhar, U.; Losic, D. One step strategy for reduced graphene oxide/cobalt-iron oxide/polypyrrole nanocomposite preparation for high performance supercapacitor electrodes. *Electrochim. Acta* **2022**, *427*, 140883. [CrossRef]
28. Tang, D.L.; Zhitomirsky, I. Pseudocapacitive properties of polypyrrole—ferrimagnetic $CoFe_2O_4$ composites. *Electrochim. Acta* **2024**, *475*, 143671. [CrossRef]
29. Thu, T.V.; Nguyen, T.V.; Le, X.D.; Le, T.S.; Thuy, V.V.; Huy, T.Q.; Truong, Q.D. Graphene-$MnFe_2O_4$-polypyrrole ternary hybrids with synergistic effect for supercapacitor electrode. *Electrochim. Acta* **2019**, *314*, 151–160. [CrossRef]
30. Alharbi, F.F.; Dahshan, A.; Ali, M.; Zeshan, M.; Henaish, A.M.A.; Ahmad, Z.; Farid, H.M.T. Study of manganese spinel ferrite/polypyrole composites for high-frequency applications. *J. Sol-Gel Sci. Technol.* **2024**, *109*, 849–858. [CrossRef]
31. Yavuz, Ö.; Ram, M.K.; Aldissi, M.; Poddar, P.; Srikanth, H. Polypyrrole composites for shielding applications. *Synth. Met.* **2005**, *151*, 211–217. [CrossRef]
32. Gabal, M.A.; Al-Harthy, E.A.; Al Angari, Y.M.; Salam, M.A.; Awad, A.; Al-Juaid, A.A.; Saeed, A. Synthesis, characterization and dye removal capability of conducting polypyrrole/$Mn_{0.8}Zn_{0.2}Fe_2O_4$/graphite oxide ternary composites. *Catalysts* **2022**, *12*, 1624. [CrossRef]
33. MacDonald, M.; Zhitomirsky, I. Capacitive properties of ferrimagnetic $NiFe_2O_4$-conductive polypyrrole nanocomposites. *J. Comp. Sci.* **2024**, *8*, 51. [CrossRef]
34. Das, K.K.; Patnaik, S.; Mansingh, S.; Behera, A.; Mohanty, A.; Acharya, C.; Parida, K.M. Enhanced photocatalytic activities of polypyrrole sensitized zinc ferrite/graphitic carbon nitride n-n heterojunction towards ciprofloxacin degradation, hydrogen evolution and antibacterial studies. *J. Colloid Interface Sci.* **2020**, *561*, 551–567. [CrossRef] [PubMed]
35. Parfimovich, I.D.; Komarov, F.F.; Milchanin, O.V.; Shchegolkov, A.V.; Tkachev, A.G. Radio absorbing composite materials of scattering type based on carbon nanotubes. *Inorg. Mater. Appl. Res.* **2023**, *14*, 962–967. [CrossRef]
36. Zhou, Y.; Chen, L.Y.; Jian, M.L.; Liu, Y.J. Recent research progress of ferrite multielement microwave absorbing composites. *Adv. Eng. Mater.* **2022**, *24*, 2200526. [CrossRef]
37. Kim, H.M.; Jeong, J.Y.; Kang, S.H.; Jin, H.J.; Choi, H.J. Dual electrorheological and magnetorheological behaviors of poly(*N*-methyl aniline) coated $ZnFe_2O_4$ composite particles. *Materials* **2022**, *15*, 2677. [CrossRef]
38. Kazantseva, N.E.; Vilčáková, J.; Křesálek, V.; Sáha, P.; Sapurina, I.; Stejskal, J. Magnetic behaviour of composites containing polyaniline-coated manganese-zinc ferrite. *J. Magn. Magn. Mater.* **2004**, *269*, 30–37. [CrossRef]
39. Stejskal, J. Interaction of conducting polymers, polyaniline and polypyrrole, with organic dyes: Polymer morphology control, dye adsorption and photocatalytic decomposition. *Chem. Pap.* **2020**, *74*, 1–54. [CrossRef]

40. Wang, W.L.; Lv, Y.P.; Liu, H.J.; Cao, Z.G. Recent advances in application of polypyrrole nanomaterial in water pollution control. *Separ. Purif. Sci. A* **2024**, *330*, 125265. [CrossRef]
41. Ul-Hoque, M.I.; Holze, R. Intrinsically conducting polymer composites as active masses in supercapacitors. *Polymers* **2023**, *15*, 730. [CrossRef] [PubMed]
42. Mandal, S.; Dasmahapatra, A.K. Hierarchical polyaniline/copper cobalt ferrite nanocomposites for high performance supercapacitor electrode. *J. Energy Storage A* **2023**, *74*, 109402. [CrossRef]
43. Alwadai, N.; Manzoor, S.; Ejaz, S.R.; Khosa, R.Y.; Aman, S.; Al-Buriahi, M.S.; Alomairy, S.; Alrowaili, Z.A.; Somaily, H.H.; Hayat, M. $CoFe_2O_4$ surface modification with conducting polypyrrole: Employed as a highly active electrocatalyst for oxygen evolution reaction. *J. Mater. Sci. Mater. Electron.* **2022**, *33*, 13244–13254. [CrossRef]
44. Stejskal, J.; Vilčáková, J.; Jurča, M.; Fei, H.J.; Trchová, M.; Kolská, Z.; Prokeš, J.; Křivka, I. Polypyrrole-coated melamine sponge as a precursor for conducting macroporous nitrogen nitrogen-containing carbons. *Coatings* **2022**, *12*, 324. [CrossRef]
45. Stejskal, J.; Sapurina, I. Polyaniline: Thin films and colloidal dispersions (IUPAC technical report). *Pure Appl. Chem.* **2005**, *77*, 815–826. [CrossRef]
46. Trchová, M.; Stejskal, J. Resonance Raman spectroscopy of conducting polypyrrole nanotubes: Disordered surface versus ordered body. *J. Phys. Chem. A* **2018**, *122*, 9298–9306. [CrossRef]
47. Jurča, M.; Vilčáková, J.; Kazantseva, N.E.; Munteanu, A.; Munteanu, L.; Sedlačík, M.; Stejskal, J.; Trchová, M.; Prokeš, J. Conducting and magnetic hybrid polypyrrole/nickel composites and their application in magnetorheology. *Materials* **2024**, *17*, 151. [CrossRef]
48. Kazantseva, N.E.; Bespyatykh, Y.I.; Sapurina, I.; Stejskal, J.; Vilčáková, J.; Sáha, P. Magnetic materials based on manganese-zinc ferrite with surface-organized polyaniline coating. *J. Magn. Magn. Mater.* **2006**, *301*, 155–165. [CrossRef]